

## **Developing New Remote Sensing Technology for More Economical Weed Control**

**Principal Investigators (PI):** Lawrence Lass and Donn Thill

**Primary PI Address:** University of Idaho, Department of Plant, Soil and Entomological Sciences. Moscow Idaho, 83844-2339.

**Primary PI Phone, Fax, Email**  
208-885-7802, 208-885-7760, and llass@uidaho.edu

**Public Abstract:** Advances in selective chemical control and application technology provide more opportunity for “smart” precision management of weeds with herbicides during crop rotations. To take full advantage of new application systems, accurate digital mapping of weed positions will be necessary. Images from multispectral and hyperspectral remote sensors maybe useful to detect and map weeds in the crop and provide guidance data for management with precision farming equipment. The objective of this project was to develop modern remote sensing procedures to identify, define, and record the locations and spatial distribution of weed infestations in wheat and pea fields with management level accuracy. The Probe 1 hyperspectral sensor, from Earth Search Sciences Inc., McCall, ID recorded images of four farms near Moscow, ID on July 19, 1998. The hyperspectral sensor has 128 bands and a spatial resolution of about 5 meters (16 feet). Classification of the images showed interrupted windgrass (*Apera interrupta* (L.) Beauv.) was detectable with hyperspectral images. Overall image error was 27% when a 3° classification angle was used. The interrupted windgrass class had an omission error of 17% (on the ground but not on the image) and a commission error of 67% (on the image but something else on the ground) when compared to the verification sites. The non-windgrass class had a 4% commission error and a 27% omission error. In comparison, the multispectral image showed few interrupted windgrass infestations, and mistakenly classified most of the pea fields as interrupted windgrass. Hyperspectral signature analysis resulted in more refined images and increased detection accuracy compared to multispectral image analysis.

**Objectives:** The objective of this project was to develop modern remote sensing procedures to identify, define, and record the locations and spatial distribution of weed infestations in wheat and pea fields with management level accuracy.

## Table of Contents

|  |    |
|--|----|
| Introduction.....  | 1  |
| A. Spectral signatures of weeds and crops. ....  | 1  |
| B. Establishing spectral development sites and ground truth verification sites. ....                     | 6  |
| B. Image rectification with ground coordinates. ....   | 8  |
| C. Image classification accuracy assessment. ....  | 9  |
| D. Weed detection with hyperspectral imagery. ....   | 10 |
| Impact of research (actual and expected) on producers.....   | 17 |
| Presentations made to producers, fieldmen, and scientist.....  | 17 |
| Education and training meetings focused on processing data for the American Farm<br>Bureau project. .... | 19 |
| Proposals written to expand the project or as a result of this project. ....                             | 19 |
| Publications: .....  | 19 |
| Software: .....  | 20 |
| Personnel:.....  | 20 |

## **Introduction**

Precision management of weeds requires accurate digital maps of their positions within fields to take advantage of site-specific application systems. Detecting and mapping weeds in crops for management with precision farming equipment may be possible with multispectral and hyperspectral remote sensing. Hyperspectral sensors split the electromagnetic spectrum between 440 and 2,543 nm into many narrow spectral bands. Visible light is 440 to 750 nm (Bennington, 1984). Depending on the type of hyperspectral sensor, the band width could range from 2 to 16 nm and the number of bands could range from 56 to 256 bands (Campbell, 1994). In comparison, most multispectral sensors have 4 to 12 bands ranging in width from 60 to 100 nm. Narrower bands allow spectral color differences between plant species to be recorded and used to separate weeds from desirable plants.

The *Probe 11* hyperspectral sensor, from Earth Search Sciences Inc., McCall, Idaho recorded images of four farms near Moscow, Idaho on July 19, 1998. The *Probe 1* is a “wiskbroom style” instrument collecting data in a cross track direction by movement of the airplane along a flight line. The instrument is an imaging spectrometer in the reflected solar region of the electromagnetic spectrum ranging from 440 to 2,543 nm. The average spectral sampling interval for visible to near infrared region (440 to 800 nm) is 16 nm and near infrared to infrared region (800 to 1,400 nm) is 13 nm. The sensor measures the spectrum in the infrared to shortwave region (1,400 to 2,543 nm) using 12 to 16 nm sampling intervals. The swath width of the instrument was 2.5 km (1.5 miles) when the aircraft is flown at 2,500 m (1.5 miles) altitude and the pixel resolution was 5 m (16 ft).

Weed infestations and field conditions were monitored and positioned with a differentially corrected global positioning system (DGPS) in 1997 and 1998. Spectral radiance measurements with a hand-held spectroradiometer were recorded for selected crops and weeds expected to appear in the images in 1997 and 1998. Farm one’s crops were winter and spring wheat and pea. Farm two’s crops were winter and spring wheat, pea, lentil, barley, and chickpea. Farm three’s crops were alfalfa, lentil, pea, chickpea, and winter wheat. Crops at the University of Idaho (UI farm) research farm were pea, lentil, winter and spring canola, winter and spring wheat, and barley.

### A. Spectral signatures of weeds and crops.

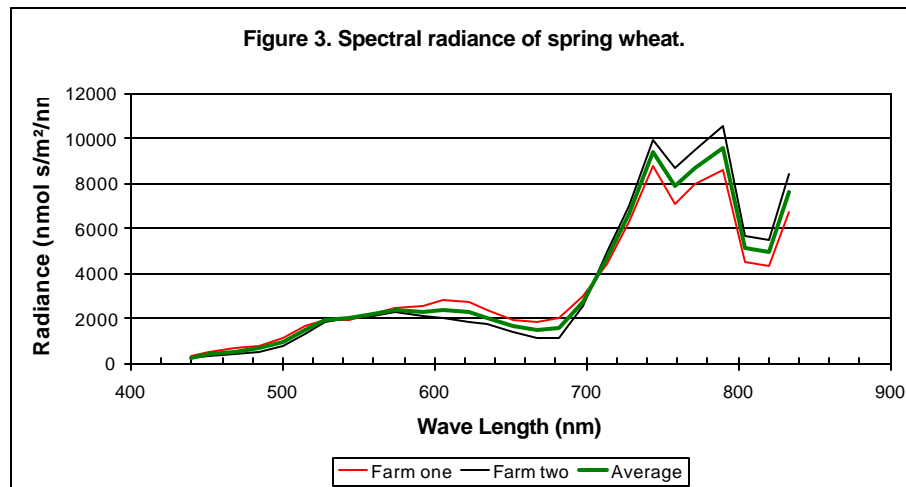
---

1 Earth Search Sciences Inc, 502 North 3<sup>rd</sup> Street, #8, McCall, ID 83638. Manufactured by Integrated Spectronics Pty Ltd, A.C.N. 003 873 443, P.O. Box 437, Baulkham Hills, NSW Australia, 2153.

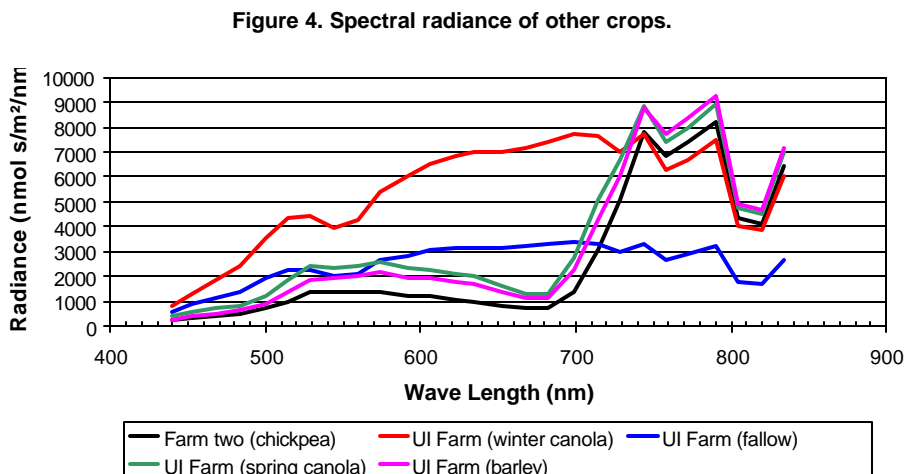


values in the near infrared range (720 to 850 nm) than senescing pea vines. Radiance values of the green vines in the area of where Photosystem I absorbs most of the light energy (600 to 700 nm) were lower than senescing vines.

The spectral radiance values of spring wheat were generally lower in 650 to 700 nm and higher in the 700 to 800 nm areas than radiance values in winter wheat (Figure 1 and 3). Spring wheat was less mature than winter wheat at the time of imaging. The characteristic valley at 540 nm and peak at 700 nm of the radiance in winter wheat is missing in the less mature spring wheat.

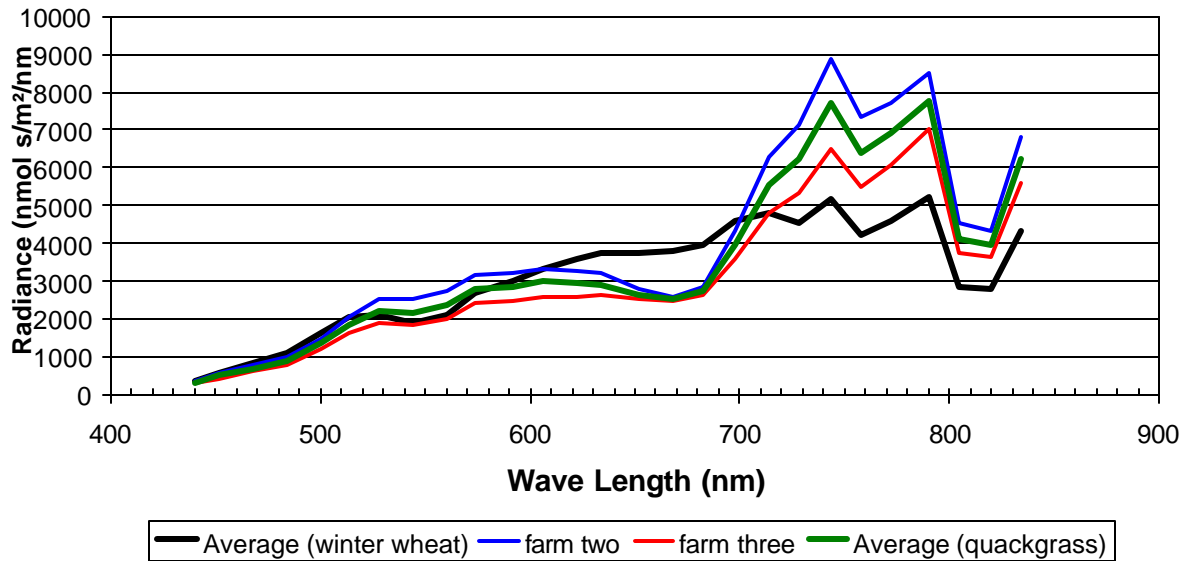


The spectral radiance of fallow ground tended to be much lower in the near infrared range (above 750 nm) (Figure 4). This confirms other studies that show near infrared is a good plant detection band. The spring planted crops had lower values in the 650 to 700 nm area than the fallow ground. The exception was winter canola that had fully senesced and was ready to harvest at the time of imaging.



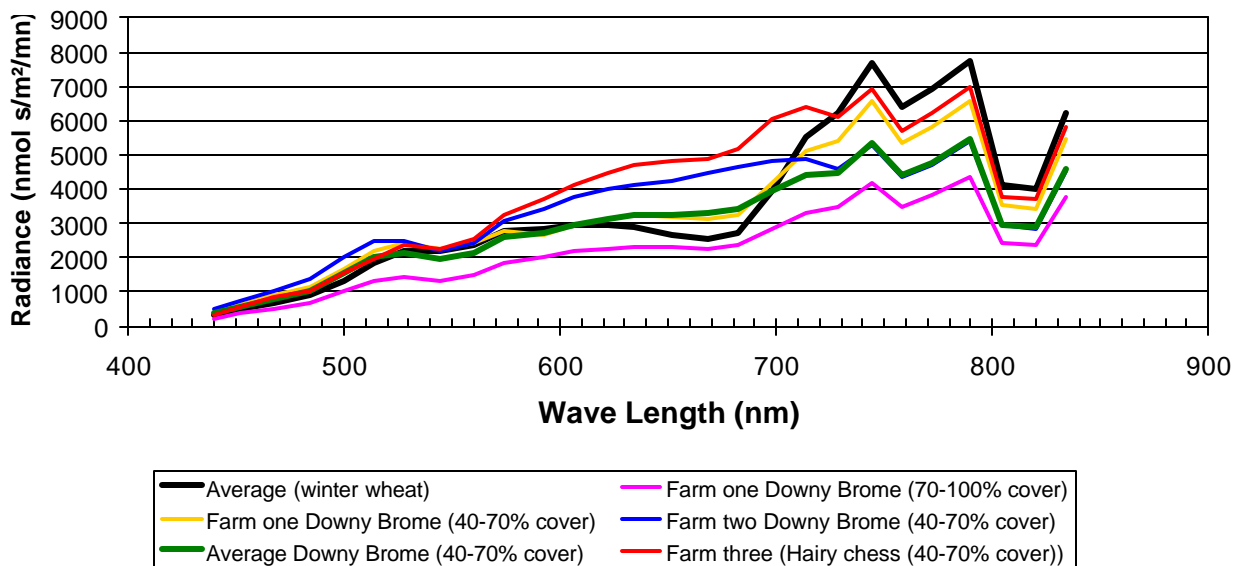
Quackgrass plants were present at farm three in two fields, but were not a major weed problem on the other farms (Figure 5). Farm two had a small infestation on one field. The quackgrass formed large patches in the wheat and represented about 40 to 70% of the vegetation cover in the infested patch. Spectral radiance values of quackgrass at 650 to 700 nm were lower than average spectral radiance of wheat (Figure 5). Image timing will play an important role in the detection of quackgrass in wheat. Quackgrass remained green after wheat had senesced.

**Figure 5. Comparison of winter wheat spectral radiance with of quackgrass at 40 to 70% cover at farm one.**



Downy brome and hairy chess had senesced at the time of imaging and spectral measurement (Figure 6). Near infrared spectral values are lower than average winter wheat values.

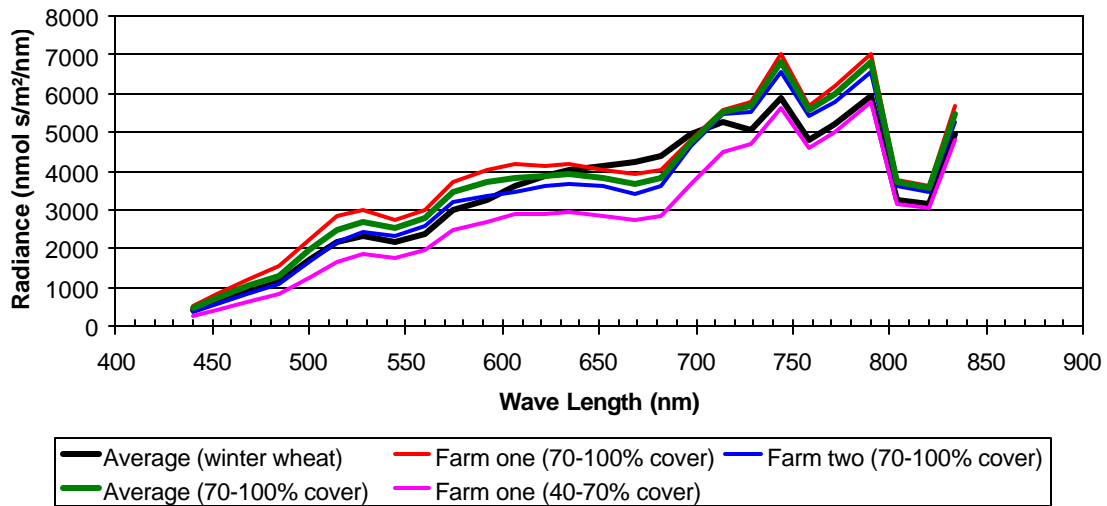
**Figure 6. Spectral radiance of downy brome and hairy chess.**



Wild oat, with a cover class of 70 to 100%, had higher spectral radiance values in the near infrared than average winter wheat and wild oat with a 40 to 70% cover class (Figure 7). The mixture of wheat and wild oat (40 to 70% wild oat) had nearly the same

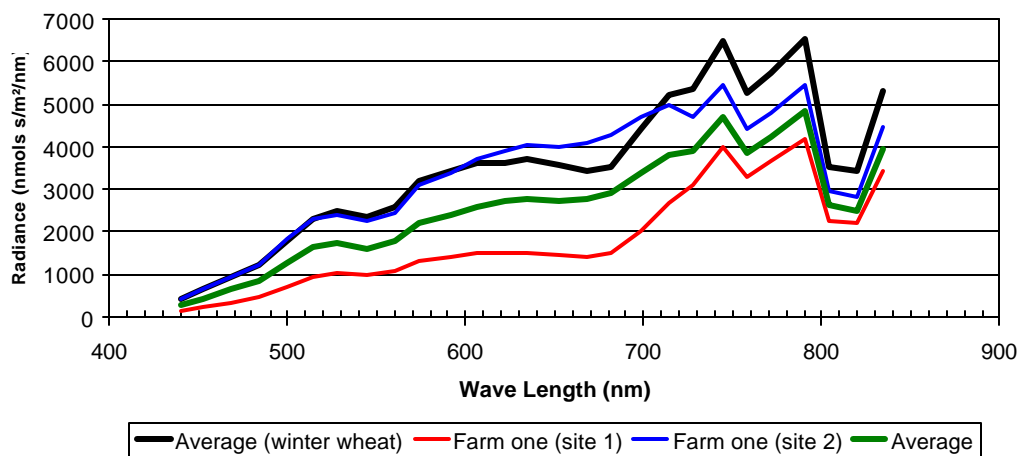
near infrared values as the average winter wheat values, but had considerably lower values in the photosynthetic range than wheat.

**Figure 7. Spectral radiance of wild oat.**



Windgrass had senesced at the time of imaging (Figure 8). Both spectral measurements were taken from areas with 70 to 100% interrupted windgrass. Variances in

**Figure 8. Spectral radiance of interrupted windgrass.**



the two windgrass locations within farm one maybe due to differences in wheat maturity, but cannot be fully explained at this time. Unfortunately, the spectral measurements of interrupted windgrass at farm two were corrupted and we were unable to collect additional data at the time of discovery.

### B. Establishing spectral development sites and ground truth verification sites.

Spectral development sites and classification verification sites were established prior to image data collection with a DGPS in June of 1998. The DGPS used point averaging to reduce the spatial error to about 2.5 m (8 ft). The spectral development sites and classification verification sites of the weeds were selected on the basis of uniform cover in one of three cover classes (low = 1 to 40%, moderate = 41 to 70%, and high = 71 to 100%). Weed species were highly variable and patches small at all three farms with the exception of interrupted windgrass on two farms. Herbicides application reduced weed infestations, in most cases, to a few sprayer skips and isolated patches (Figure 9 to 11).

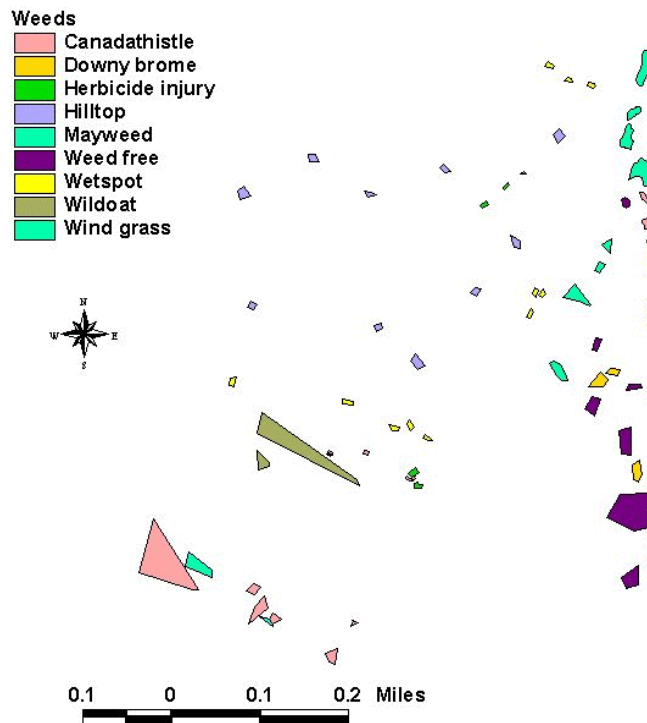


Figure 9. Farm 1 Weed Map.



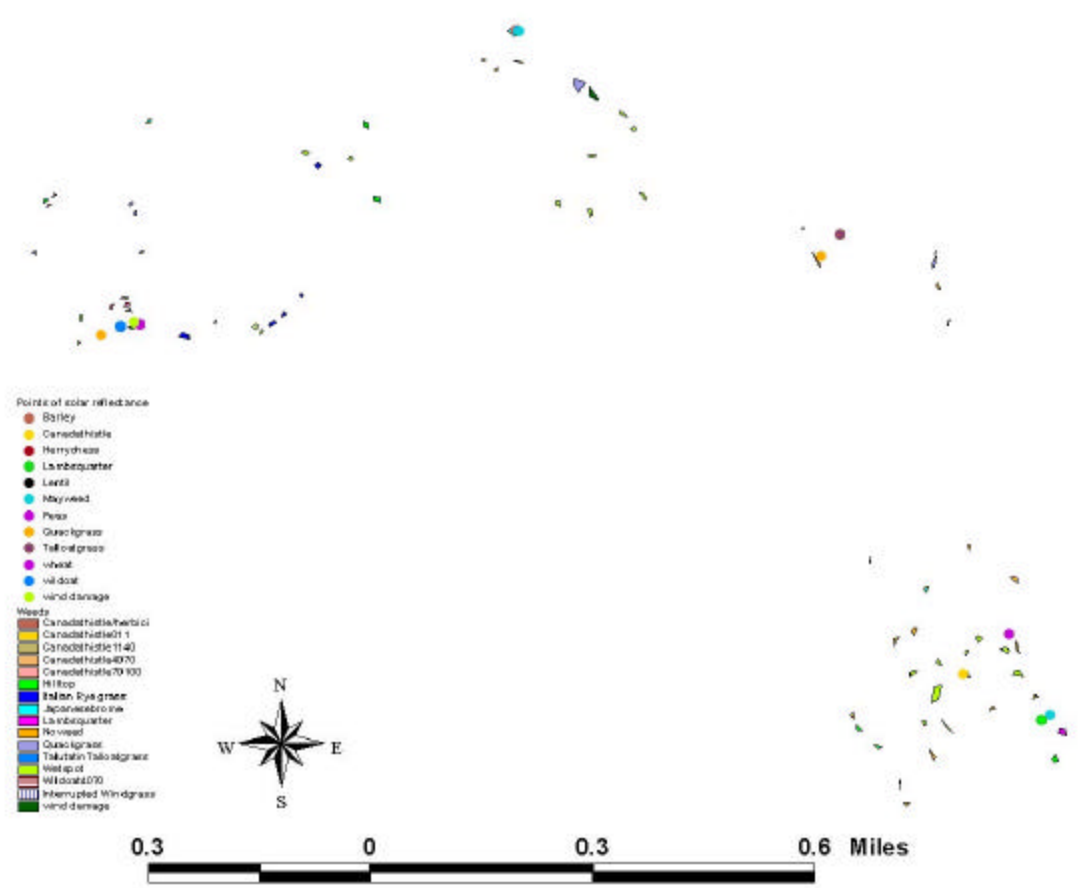
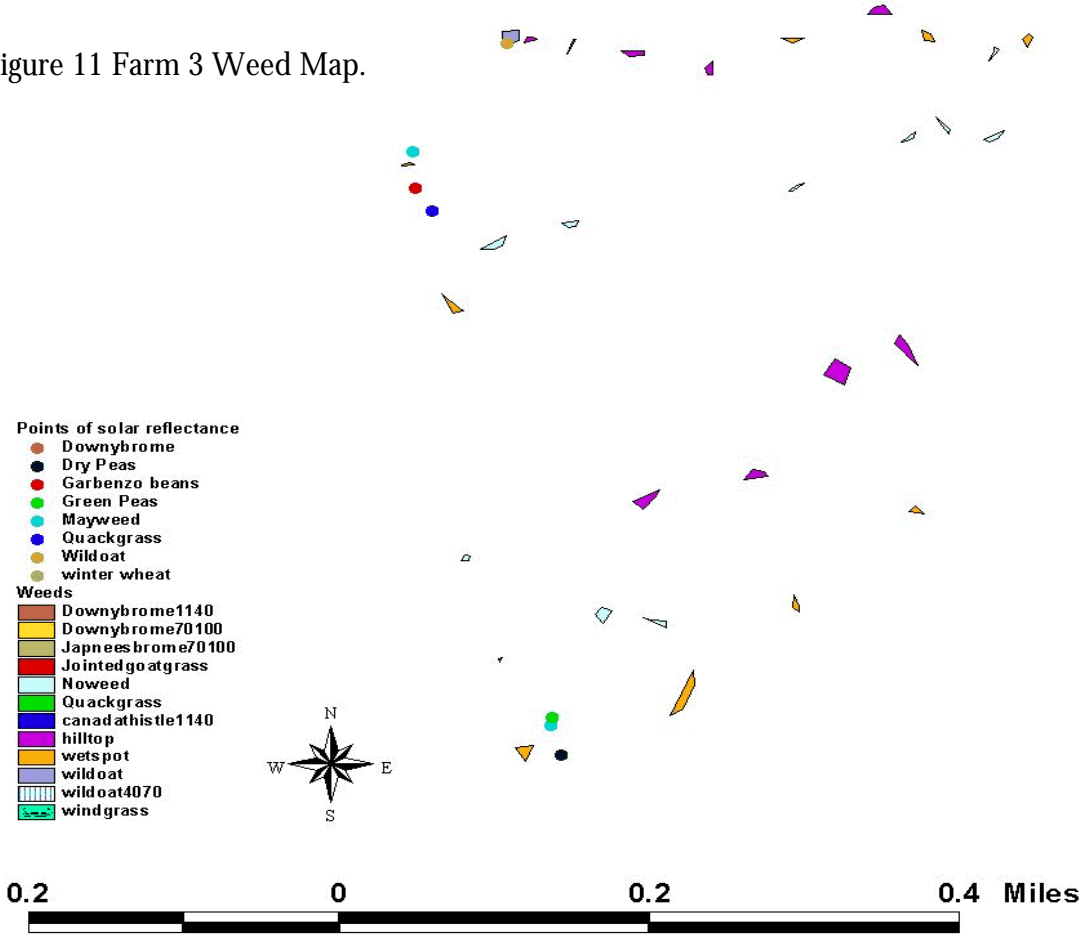


Figure 10 Farm 2 Weed Map

Figure 11 Farm 3 Weed Map.



### C. Image rectification with ground coordinates.

Attempts to rectify the images with ground control points to allow statistical comparison with GPS positioned weed locations have been unsatisfactory using traditional rubber-sheeting georectification methods. Two problems with the detector flight platform came into play. Airplane mounted equipment seldom can fly in a straight line and at the same speed over a given distance. Pixel sizes ranged from 4.3 to 5.2 m in a single flight line. Flight lines were from south to north, but could vary 1 to 30 pixels east or west depending on the crosswinds and thermal updrafts. Rubber sheet methods of rectification accurately rectify the parts of the flight line that do not deviate from the flight plan and air speed, but fail where the deviation occurred. Multiquadratic rectification algorithms used to rectify other whiskbroom type remote sensing equipment are being adapted and modified to correct the hyperspectral images.

This project developed software (*Image Rectifier2*) to use the onboard GPS unit to

determine the necessary correction for flight path variation (pitch, roll, yaw, and flight speed variations). During the flight, the *Probe* sensor attempts to keep the scan lines parallel by electronically leveling and rotating the instrument. This will introduce an image warp where the true corners do not form a 90° rectangle as represented in the raw data, but rather form a parallelogram. This warp was correctable with traditional quadratic georeferencing to ground control points. These control points have been determined with DGPS and from a Digital Orthophoto Quads (DOQ).

After registration, images from farm one had a position error of 1.2 m (3.8 ft). Building and roads features on the registered image of farm one precisely overlaid data taken with the DGPS. Images of farm two had a position error of 212 m (678 ft) to the north and 153.9 m (490 ft) to the west when compared to known points on the ground after registration. Image coordinates of farm two were offset so the image coordinates of roads and intersections matched the true ground coordinates. This reduced the position error of the farm two images down to 5 m (16 ft), but did not totally remove it. Farm 3 could not be rectified because of an unstable aircraft due to cross winds and was not usable for image classification.

D. Image classification accuracy assessment.

Accuracy assessment of image classification is often represented in the form of an error matrix that contrasts image classification with ground truth data (Card, 1982, Congalton, 1991, Congalton, et al., 1983, and Goodchild and Gopal, 1989). The rows of this contingency table represent the classified image categories and the columns denote ground truth categories ( $N_i$ ,  $N_j$  and  $N$  denote row, column, and grand totals  $i=1, 2, 3, \dots, C$ ), respectively:

|                     |          | <b>Ground Truth</b>        |                            |                            |     |                            |                            |
|---------------------|----------|----------------------------|----------------------------|----------------------------|-----|----------------------------|----------------------------|
|                     |          | <b>1</b>                   | <b>2</b>                   | <b>3</b>                   | ... | <b>C</b>                   |                            |
| <b>C</b><br>l<br>as | <b>1</b> | $x_{11}$                   | $x_{12}$                   | $x_{13}$                   | ... | $x_{1c}$                   | <b><math>N_{1.}</math></b> |
|                     | <b>2</b> | $x_{21}$                   | $x_{22}$                   | $x_{23}$                   | ... | $x_{2c}$                   | <b><math>N_{2.}</math></b> |
|                     | <b>3</b> | $x_{31}$                   | $x_{32}$                   | $x_{33}$                   | ... | $x_{3c}$                   | <b><math>N_{3.}</math></b> |
|                     | ...      | ...                        | ...                        | ...                        | ... | ...                        | ...                        |
|                     | <b>C</b> | $x_{c1}$                   | $x_{c2}$                   | $x_{c3}$                   | ... | $x_{cc}$                   | <b><math>N_{c.}</math></b> |
|                     |          | <b><math>N_{.1}</math></b> | <b><math>N_{.2}</math></b> | <b><math>N_{.3}</math></b> | ... | <b><math>N_{.c}</math></b> | <b>N</b>                   |

Measures of agreement were calculated between ground truth and classification data to determine omissions ( $\mathcal{O}_i$ ) and commissions ( $\mathcal{C}_i$ ) error rates for class  $i$  defined as:

$$\mathcal{O}_i = (1 - x_{ii}/N_{i.}) \text{ and } \mathcal{C}_i = (1 - x_{ii}/N_{.i})$$

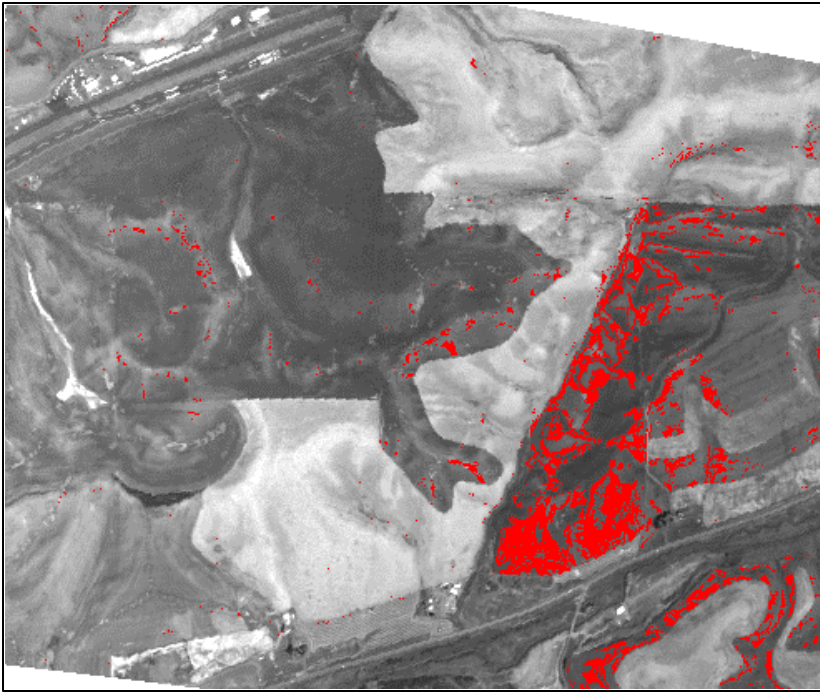
where the marginal proportions are  $x_{ii}/N_{i.}$  and  $x_{ii}/N_{.i}$ . The omission error indicates the proportion of a cover class not on the image but present on the ground. The

omissional error indicates the proportion of a cover class on the image, but not present on the ground. If a precision sprayer were to use these images for guidance, the omissional error would cause the sprayer to skip areas with the weed and the commission error would cause areas to be sprayed without the weed. Considering  $x_{ii}/N_i$  and  $x_{ii}/N_i$  as binomial and conditional binomial variates, respectively, Bayesian posterior distributions for  $\Theta_i$  and  $\mathcal{C}_i$  can be developed following procedures given by Shafii, et al., 1998. Subsequent contrasts of spectral angles and unsupervised classification can then be made to determine probable differences among  $\Theta_i$  and  $\mathcal{C}_i$  values.

#### E. Weed detection with hyperspectral imagery.

The weed studied in this project was interrupted windgrass, which is a winter annual grass found in the major cropping regions of the Pacific Northwest. Interrupted windgrass infestation patterns in winter wheat fields vary from randomly scattered plants to large dense patches. This weed also maybe found in bare areas of perennial crops such as Kentucky bluegrass and alfalfa. Occasionally interrupted windgrass is found in spring crops, where late germinating plants have avoided cultural and chemical controls. Windgrass plants generally overtop winter wheat by about 15 cm (6 inches) at maturity. Although the weed is widely established it tends to become a problem in the wetter locations of a field due to cultivation avoidance during spring cropping years, but is known to invade dry areas where crop competition is poor.

Areas known to be infested with interrupted windgrass appeared on the images of farm one and farm two as unique pixel values when classified with the SAM algorithm. A postemergence herbicide was used to spot-treat areas of interrupted windgrass at farm two. Spray patterns showing no windgrass appeared on the images where the treatments were applied. The images showed windgrass free strips where the sprayer was left on while being driven between more densely infested sites (Fig 12 points a and b).

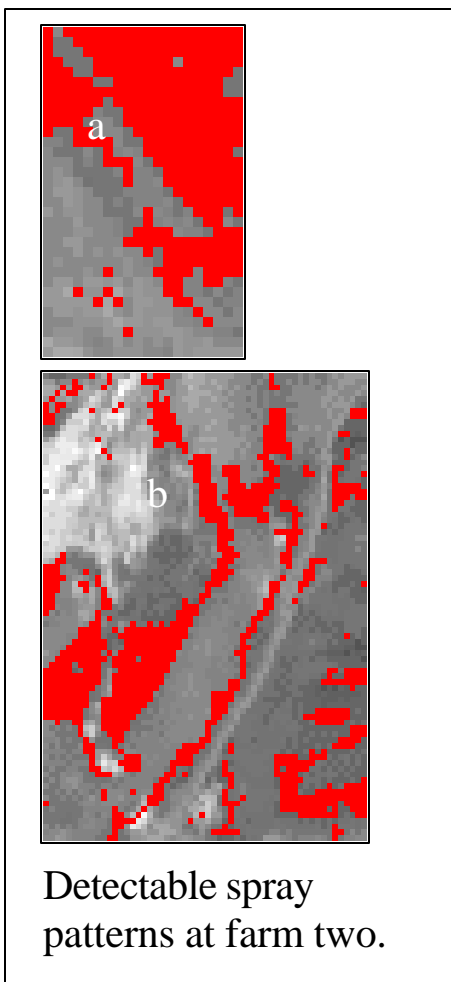


# Farm one

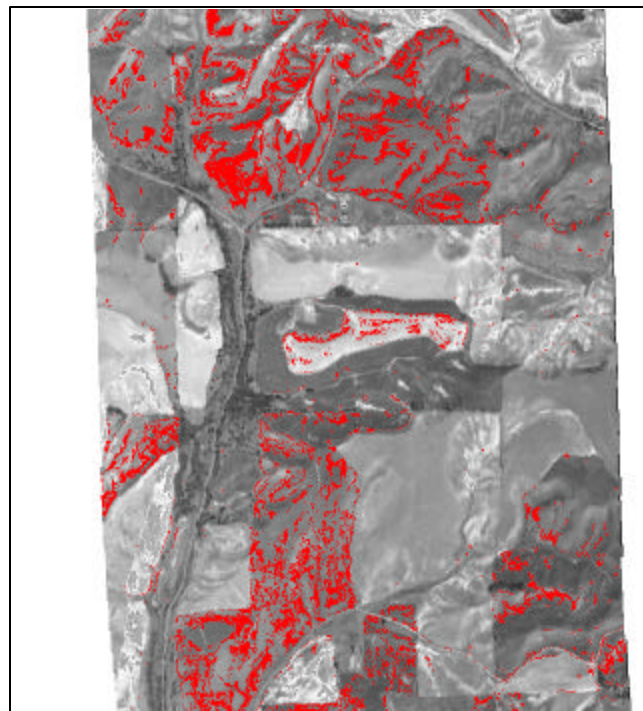


500 m  
1600 ft

North



Detectable spray  
patterns at farm two.



500 m

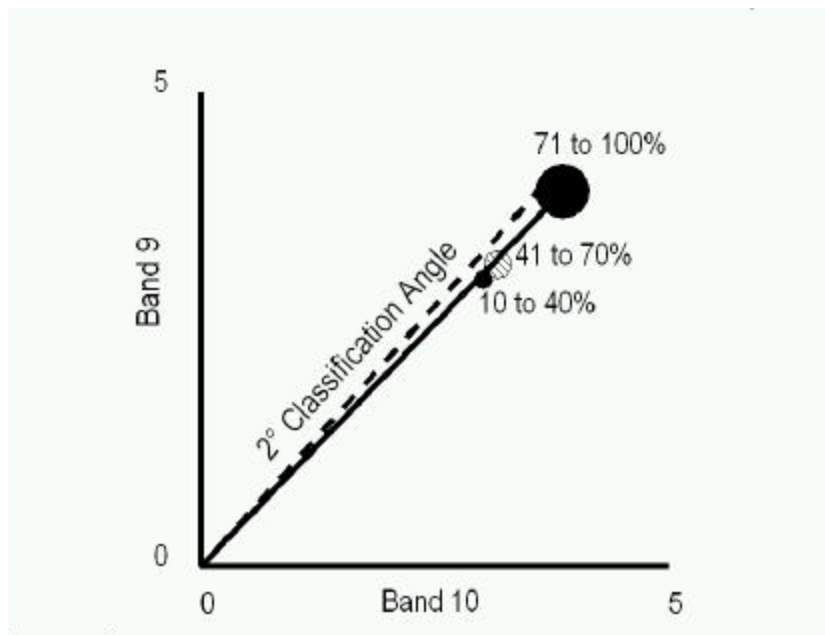


North

# Farm two

Fig. 12 Hyperspectral image showing interrupted windgrass (red).

The image generated from the high cover class signature file showed the low and moderate verification sites were also being detected. This indicates the spectral angle of the high cover class could identify interrupted windgrass regardless of cover class range (10 to 100%). The SAM algorithm is a minimum angle procedure that assumes a set of signatures are the same if they fall along a line connected to the origin of the band space (Figure 2). SAM



treats the signature value as a vector. If the angle formed by an

unknown pixel and the origin falls within the threshold classification angle (i.e. 2 to 5°) of a known class the unknown pixel is assigned to the known class. The SAM algorithm compensates for significant variations in illuminations by assuming different light conditions will lead to a set of signatures that fall along a line connected to the origin of the band space (Figure 2). As the density of interrupted windgrass decreased, the signature values tended to stay within 1° of the vector made by the high cover class when connected to the origin. The lowest cover class of interrupted windgrass tended to be slightly below the vector through the center of the highest class. The shift towards the pure wheat signature was expected because the lowest class of interrupted windgrass would have 60 to 90% winter wheat cover. The SAM algorithm was not able to separate different cover classes of interrupted windgrass because the same angle was made by the three cover classes. This was further tested by using the highest cover class to reclassify farm one images with the best (3°) classification angle based on accuracy assessment. Area analysis of the classified images using the high cover class signatures showed the same total infested area (57 ha or 141 acres) as if the images were classified with signatures developed from the three cover classes.

Visual interpretation of the images from farm one showed major interrupted windgrass infestations appear regardless of the classification angle used, but the lowest angle (2°) did not

completely define the extent of the infestation when compared to known infestations, while the highest spectral angle ( $5^\circ$ ) improved the boundary definition, but started to show new areas that were not infested. Area analysis of farm one shows that 21, 57, 122, and 199 ha or 51, 141, 302, and 493 acres of interrupted windgrass could be detected when a 2, 3, 4, and  $5^\circ$  angle, respectively, was used in the SAM algorithm (Table 1). Likewise at farm two, area analysis of the images showed more of the area infested

Table 1. Area analysis of hyperspectral images classified with spectral angle mapper algorithm of 1 near Moscow, Idaho acquired on July 19, 1998.

| Metric Units          | Farm One                       |       |       |       | Farm Two                       |       |       |       |
|-----------------------|--------------------------------|-------|-------|-------|--------------------------------|-------|-------|-------|
|                       | Classification Angle, $^\circ$ |       |       |       | Classification Angle, $^\circ$ |       |       |       |
|                       | 2                              | 3     | 4     | 5     | 2                              | 3     | 4     | 5     |
|                       | ------(ha)-----                |       |       |       | ------(ha)-----                |       |       |       |
| Interrupted windgrass | 21                             | 57    | 122   | 200   | 8                              | 116   | 216   | 370   |
| Non-windgrass         | 863                            | 827   | 762   | 684   | 1,483                          | 1,375 | 1,275 | 1,121 |
| Image area            | 884                            | 884   | 884   | 884   | 1,491                          | 1,491 | 1,491 | 1,491 |
| English Units         | ------(acres)-----             |       |       |       | ------(acres)-----             |       |       |       |
| Interrupted windgrass | 51                             | 141   | 302   | 493   | 21                             | 286   | 533   | 914   |
| Non-windgrass         | 2,133                          | 2,043 | 1,882 | 1,691 | 3,663                          | 3,398 | 3,151 | 2,770 |
| Image area            | 2,184                          | 2,184 | 2,184 | 2,184 | 3,684                          | 3,684 | 3,684 | 3,684 |

with interrupted windgrass as the classification angle increased (Table 1). Increasing the classification angle to  $30^\circ$  showed all of the imaged area as infested in farm one and farm two. Understanding area analysis and selection of the appropriate classification angle requires accuracy assessment to determine the image with the lowest classification error.

The overall image error for farm one was 19% for the  $2^\circ$  classification angle, and the image error increased about 7% for each degree increase in classification angle (Table 2). Upper and lower probability limits of the overall image error for farm one did not overlap with the other classification angles, indicating that the four angles used for image classification were significantly different ( $p = 0.05$ ). The overall image error for farm two was 7, 14, 19, and 32% for the 2 to  $5^\circ$  classification angles, respectively. Images classified with  $3^\circ$  and  $4^\circ$  angles have overlapping of upper and lower probability bounds indicating that in this case images were statistically the same. However, these images were different from images using  $2^\circ$  and  $5^\circ$  angles (Table 2). Overall image error indicates farm one spectral values of interrupted windgrass were different from the other features measured in the field, but when used at farm two the interrupted windgrass signature produced the same results with  $3^\circ$  and  $4^\circ$  classification angles. This would suggest the reflectance of interrupted windgrass on farm two had a bimodal distribution, probably due to the late maturing interrupted windgrass. Developing extensive library based signature files and models predicting signature shift at different growth stages may be necessary

to fully utilize hyperspectral sensors to detect plant species.

The 3° classification angle provided the best blend of omission and commission errors for precision sprayer applications. The classification procedure found 57 ha (141 acres) interrupted windgrass in the farm one image (884 ha or 2,148 acres) (Table 3). The classified image of farm two showed 116 ha (286 acres) interrupted windgrass (Table 3). A precision application treating only the infested area on the image would reduce interrupted windgrass control costs by more than 95% for farm one and 92% for farm two compared to traditional broadcast treatment of the area. Accuracy assessment of the 3° classification angle showed the images from farm one omitted 9 ha (22 acres) in the 844 ha (2,148 acres) image or 16% of all interrupted windgrass found in the image area (Table 3). The omission error would cause the precision sprayer to skip 9 ha (22 acres) at farm one, but would manage 99% of the area imaged. If the spectral angle was increased to 5° the skip at farm one would be reduced to 2 ha (5 acres), but a larger area would need to be sprayed (200 ha or 493 acres). At farm two, the commission error of the 3° classification would cause the precision sprayer to skip 65 ha (161 acres) in the 1,491 ha (3684 acres) image or 56% of all interrupted windgrass. Increasing the spectral angle to 5° will reduce the skip to 59 ha (146 acres) at farm two and would manage 96% of the image area for interrupted windgrass.

Accuracy assessment also shows the amount of over commitment (commission error) by the classification procedure when detecting interrupted windgrass. The commission error represents areas where the image data indicates the precision sprayer should turn on, but a non-windgrass feature would be sprayed. The 3° classification of the farm one image over committed by 66% or 38 ha (94 acres) and farm two image commission error was 77% or 89 ha (219 acres). More than half the commission error of the 3° classification angle from both farms came from verification sites heavily infested with wild oat. Lowering the classification angle would reduce commission error, but increases omission error (Table 3). Traditional weed management strategies would broadcast spray regardless of the presence or absence of interrupted windgrass. The commission error would cause the precision spray equipment using the images for application guidance to treat a small area, in this case about 5%, as if being managed traditionally with a broadcast application.

In comparison to the hyperspectral images classified with SAM, the more traditional method of multispectral remote sensing using unsupervised classification with principle component analysis (PCA) of 12 bands (440 to 1085 nm) showed the overall image error of the farm one image was 53% and farm two was 21% (Table 3). The omission error for interrupted windgrass from the PCA image of farm one was 30% and farm two was 76%. The commission error for interrupted windgrass of farm one was 82% and farm two was 90% (Table 3). PCA images confused pea fields with interrupted windgrass infestations at both farms. The pea vines were dry and visibly about the same yellow-tan as the interrupted windgrass at the time of the flight. Costs of data acquisition for multispectral images having 4 to 15 bands are about one-third the cost of hyperspectral image data, but in this study the accuracy of hyperspectral image data was about two times more accurate than the 3° classification angle.



This study showed interrupted windgrass infestations were detectable at management level precision for computer control application equipment in winter wheat at two farms with hyperspectral sensor technology. The 3° classification angle provided the best interrupted windgrass detection with lowest combined omission and commission error rates. The late flight date, July 19, imaged nearly mature windgrass, therefore current year management was not practical. The maps generated by the imagery could be utilized for management in the other rotational cropping years. Successful current year management will require images of seedling weeds, but data acquisition may be hampered by cloud cover earlier in the year and by smaller plants (less reflective surfaces). The hyperspectral analysis of the Probe 1 using the spectral angle mapper were more accurate than multispectral PCA analysis where the PCA images showed a few interrupted windgrass infestations in the correct locations, but mistakenly classified most of the pea fields as the weed. Results of this study show image data from hyperspectral sensors to be the preferred when detecting interrupted windgrass.

### **Impact of research (actual and expected) on producers.**

This work supports producer-identified short- and long-term solutions to weed management with precision application equipment. It has resulted in a working example of a procedure for remote sensing to detect, identify, delineate, quantify, and produce both electronic and paper map records of small colonies of individual weed species in wheat and peas. It showed expected levels of precision for detection, and show how to optimize remote sensing for managerially meaningful detection of weeds in wheat and peas. Currently, large producers and cooperatives of high value vegetable and fruit crops are positioning to purchase and classify hyperspectral images. Continued research will be necessary to reduce processing time and classification costs to make it practical for small producers.

### **Presentations made to Producers, Fieldmen, and Scientist.**

1997

Lass, L. W. and D. C. Thill 1997. Presentation to 65 producers and field men at the University of Idaho, Weed Science Field Tour, June, 1997. Described the American Farm Bureau project and demonstrated and time line.

Lass, L. W. and D. C. Thill 1997. Presentation to 324 producers and agricultural consultants at University of Idaho, Dept. of Plant, Soil & Entomological Sciences Field Day. Showed examples of remote sensing, demonstrated light spectra with filters and sensors, provided global positioning training, and described the American Farm Bureau project.

Lass, L. W. and D. C. Thill 1997. Presentation to 70 producers at Wilbur-Ellis Co. Field Day. Describing the American Farm Bureau project.

Lass, L. W. and D. C. Thill 1997. Presentation to 32 producers of spectral radiance of weed and crops at University of Idaho, Nez Perce County Extension Education Meeting

Lass, L. W. and D. C. Thill 1997 Poster presentation and talk to Idaho Farm Bureau about the research project.

#### 1998

Lass, L. W. and D. C. Thill. 1998. Poster presentation of statistical procedure developed to assess remote sensing image accuracy for the American Farm Bureau Project. Weed Science Society of America

Lass, L. W. and D. C. Thill. 1998. Symposium on Remote Sensing and GPS. (Used spectral radiance data from American Farm Bureau project for my presentation). Western Society of Weed Science

Lass, L. W. and D. C. Thill. 1998. Presented Preliminary results of the hyperspectral data to the Idaho Farm Bureau Business meeting in McCall, Idaho

#### 1999

Lass, L. W. and D. C. Thill 1999 Poster presentation to American Farm Bureau Meeting, Albuquerque, NM.

Abstract: Precision management of weeds requires accurate digital maps of their positions within fields to take full advantage of site-specific application systems. Multispectral and hyperspectral remote sensing make it possible to detect and map weeds in the crop for management with precision farming equipment. The Probe 1 hyperspectral sensor, from Earth Search Sciences Inc, McCall, ID, splits the visible and near-infrared spectrum into 128 narrow bands instead of the three to seven bands typically used by multispectral sensors. This project used images from the Probe 1 sensor to detect, delineate, and measurement of multiple species of weeds in wheat and pea.

Lass, L. W. and D. C. Thill. Poster presentation producers, farmers, and Scientist at the Western Society of Weed Science, Colorado Springs, CO

Abstract. Advances in selective chemical weed control and application technology provide more opportunity for “smart” precision management with herbicides during crop rotations. To take full advantage of new application systems, accurate digital mapping of weed positions will be necessary. Digital maps generated from images using multispectral and hyperspectral remote sensors offer a rapid method of surveying the weeds in the field. The objective of this project is to develop modern remote sensing procedures to identify, define, and record the locations and spatial

distribution of weed infestations in wheat and pea fields with management level accuracy. The Probe 1 hyperspectral sensor, from Earth Search Sciences Inc., McCall, ID recorded images of four farms near Moscow, ID on July 19, 1998. The hyperspectral sensor has 128 bands and a spatial resolution of about 5 m. Images were georectified using both flight line correction and quadratic rectification algorithms. Images are currently being processed to develop spectral signatures for the training sites. Preliminary classification of the interrupted windgrass spectral signature indicates hyperspectral signature analysis enhanced the detection when compared to a multispectral image. The multispectral image showed a few interrupted windgrass infestations with a cover class 70 to 100%, but mistakenly classified most of the pea fields as interrupted windgrass. Hyperspectral signature analysis of interrupted windgrass generated an image with an omission error of 29% and a commission error of 1%. Hyperspectral signature analysis allowed us to refine the images and increase detection accuracy.

Field Day for the Dept. of Plant, Soil, and Entomological Sciences at the U. of I. Presentation to 352 farmers and fieldmen of research result of the American Farm Bureau Project. Showed poster, described results and answered questions.

### **Education and training meetings focused on processing data for the American Farm Bureau project.**

Lass, L. W. 1999 Attended American Soc. of Photogrammetric Engineering & Remote Sensing, Portland, OR for training focused on using atmospheric correction to enhance hyperspectral classification.

Lass, L. W. 1999. International Society of Remote Sensing, Las Vegas for training focused on using hand held spectrometers to enhance hyperspectral classification.

### **Proposals written to expand the project or as a result of this project.**

Making hyperspectral images usable for detecting weeds in rangeland and forest. /USDA NRICGP. 1998. Not funded.

Remote sensing mountain gorilla habitat in Rwanda for the National Geographic. / National Geographic. Funded.

Understanding the fundamentals of weed dynamics on an ecosystem scale. /USDA NRICGP. 1999. Not funded.

### **Publications:**

1. Lass, L. W., D. C. Thill, and B. Shafii. 2000. Developing new remote sensing technology for detecting interrupted windgrass (*Apera interrupta*) in cropland. Weed Technology. In review.
2. Lass, L.W., B. Shafii, W.J. Price, and D.C. Thill. 2000 Assessing agreement in multispectral images of yellow starthistle (*Centaurea solstitialis*) with ground truth

data using a Bayesian methodology. Weed Technology In Press.

3. Price, W.J., B. Shafii, L.W. Lass, and D.C. Thill. 1998. Assessing Variability of Agreement Measures in Remote Sensing using a Bayesian Approach. Appl. Stat. in Ag., p. 43-54.

### **Software:**

Georectifier 1.0. An image rectification program that shifts scan lines to match GPS readings.

ProbBounds 1.0 An image accuracy assessment program that develops Bayesian posterior distributions for omissions and commissions error matrix.

### **Personnel:**

| Name          | Position  | Status | Time                      | Paid |
|---------------|-----------|--------|---------------------------|------|
| Donn Thill    | Faculty   | F      | 5%                        | O    |
| Lawrence Lass | Technical | F      | 25%                       | AFB  |
| Adnan Zahoor  | Student   | NC     | 3 Months<br>(summer help) | AFB  |
| Tim Gautier   | Student   | N      | 37%                       | AFB  |
|               |           |        |                           |      |

### **Other Funding:**

|   |        |
|---|--------|
| BLM   | 45,661 |
| American Farm Bureau Foundation for Agriculture | 44,638 |
| USFS  | 5,000  |